Numerical investigation of the effects of friction and heat transfer on a non-premixed Rotating Detonation Combustor operation

Pierre Hellard, Thomas Gaillard, Dimitry Davidenko, Ratiba Zitoune, Pierre Vidal

Numerical investigation of the effects of friction and heat transfer on a non-premixed Rotating Detonation Combustor operation

P. Hellard*[1], T. Gaillard[1], D. Davidenko[1], R. Zitoun[2], and P. Vidal[2]

[1]DMPE, ONERA, Université Paris Saclay, F-91123 Palaiseau, France
[2]Institut Pprime, UPR 3346 CNRS, Fluid, Thermal and Combustion Sciences Dpt, ENSMA, 86360 Chasseneuil-du-Poitou, France

Abstract

Rotating Detonation Combustors (RDC) are a promising solution for increasing the thermal efficiency of engines. The high temperature and pressure caused by detonation induce a high exchange at the combustor walls, which, in turn, can affect detonation propagation. This numerical study investigates the viscous wall effects on detonation propagation and engine performance based on high-fidelity simulations of an experimental RDC currently being prepared for testing. The results show that the wall effects reduce the detonation velocity by only 2% and that the wall heat flux can be as high as 17 MW/m² in the detonation propagation zone.

Keywords: *Rotating detonation combustor, Heat flux, Mixing, Deflagration, Large Eddy Simulation, Hydrogen*

Introduction

Detonation-based combustors attract attention because they potentially increase the thermal efficiency of power generation systems. Most of the concepts focus on the Rotating Detonation Combustor (RDC). As presented schematically in Figure 1, an RDC is often composed of an annular chamber in which one or several detonations continuously propagate while consuming the propellants injected at the chamber entry between two detonation passages. RDCs have a higher compacity than current constant-pressure combustors due to the reduced length of the chamber and the very short reaction time of the detonation process. The pressure in the chamber and the number of detonation fronts usually increase with increasing the injected mass flow rate [1]. Indeed, detonation fronts in gases have a cellular structure, and the mean width of the detonation cells is proportional to the reaction length. The smaller the cell width, the shorter the reaction length, so the detonation propagation is all the easier if the mean width of the detonation cells is small [2] because this width decreases with increasing the initial pressure. Using detonation also theoretically produces a total pressure gain in the combustor thus reducing the need for a high-pressure ratio compressor in the case of air-breathing applications.

On the experimental side, Wolański [3] attached a helicopter turbine to an experimentally optimized RDC and achieved a 5 to 7% reduction in specific fuel consumption compared to the original combustor. Naples et al. [4] also showed that an RDC attached to a commercial turbine can achieve comparable or better performance than a conventional combustor.

Fewer results are available about the efficiency increase in rocket-based RDCs (also referred to as RDREs for Rotating Detonation Rocket Engines). Fotia et al. [5] compared the propulsive performance of different nozzles attached to an RDC, but there are no comparisons to conventional rocket engines. The RDC experiments of Frolov et al. [6] showed that RDRE can achieve good performance at low chamber pressure, as predicted in the numerical study of Davidenko et al. [7].

One of the challenges with RDCs is to demonstrate a long-duration operation because of the high pressure and thermal loads. Therefore, most test runs last less than one second in uncooled combustors to limit the wall temperature increase. For example, Randall et al. [8] measured wall temperatures of 1000 K after 2 seconds of operation in an H_2/O_2 RDC. Wall heat flux is difficult to predict as they depend on multiple factors, including the RDC configuration. Goto et al. [9] showed that the wall heat flux increases with the combustion efficiency, depending on the injector geometry,

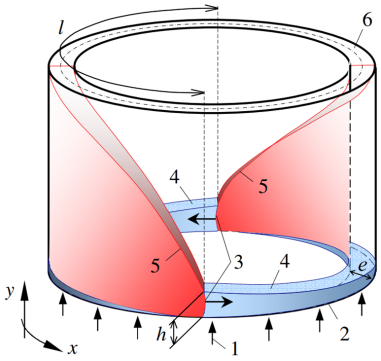

Figure 1: Scheme of an RDC with two co-rotating detonation waves. 1: Injected fresh mixture, 2: injector surface, 3: detonation waves, 4: fresh-burned gases contact surface, 5: oblique shock wave

*Corresponding author: pierre.hellard@onera.fr

and with increasing the mass flow rate. Several studies have dealt with heat flux measurements in air-breathing RDCs [2][10] and reported heat loads varying between 1 and 8 MW/m². The wall heat flux is not uniform along the channel [11] and reaches a maximum around the detonation wave height. Obtaining experimental data on heat loads on the inner and outer walls at multiple locations would require more sensors.

High-fidelity 3D simulations could help to obtain heat flux distributions over the chamber walls. Most published 3D RDC simulations assume adiabatic walls [12][13][14][15][16] because it would require highly refined mesh at the walls to resolve the boundary layer. High-fidelity simulations sometimes overpredict the detonation velocity compared to experiments [17][16], and the discrepancy is sometimes attributed to the neglected wall heat flux [16]. Among the few attempts to study wall heat flux numerically, Wang et al. [18] performed URANS simulations of an RDC using premixed H_2/air. A wall law function was used to model the viscous interactions at the wall. The calculated heat flux reaches a peak value of 80 MW/m² in the detonation front on the most refined mesh, which seems quite high compared to values found in the literature. Wu et al. [19] showed that the assumed wall temperature fixed in the simulation has little effect on the wall heat flux for wall temperatures of 600 and 900 K. Simulations of a premixed H_2/air RDC were also performed by Cocks et al. [20] with and without wall viscous interactions. A hybrid RANS/LES approach was used with a refined mesh at the wall ($y^+ < 10$). The paper shows that viscous interactions at the wall change the RDC performance, but not the detonation velocity, which actually increases when the wall heat flux is considered. This last result was not expected since theoretical work on detonation propagation showed that friction and heat transfer reduce detonation velocity [21][22].

This study is a sensitivity analysis of the viscosity and heat-transfer interactions at the RDC wall with a numerically optimized injector for non-premixed propellants. Section 1 discusses the numerical methods and the geometry studied, and Section 2 summarizes the analysis of the flow field structure, detonation velocity, mixing quality, and wall heat load.

1 Numerical modeling

The computational domain is a quarter of an experimental RDC of the PROMETEE facility of the Pprime Institute. The RDC has an inner diameter of 70 mm, an annular gap of 5 mm, and a length of 60 mm. Simulating only a quarter of the RDC is equivalent to assuming four co-rotating detonations in the RDC and helps to reduce the computational cost. The purpose here is not to compare experimental and numerical results.

The RDC injector designed for this study consists of multiple injection elements arranged periodically along the circumference of the RDC. The injection element (hereafter referred to as *TripHy*) is a O_2/H_2/O_2 triplet configuration, with eighteen *TripHy* injection elements on a quarter of the injector. The total mass flow rate, $\dot{m}_{tot}$ in the chamber is 120 g/s, corresponding to a mass flux of 100 kg/m²/s through the chamber cross-section.

The Large Eddy Simulations (LES) presented below are performed with the CEDRE code developed at ONERA. The code solves the Navier-Stokes equations for compressible reactive flow on general unstructured meshes with the CHARME solver. A MUSCL (Monotonic Upstream Scheme for Conservation Laws) scheme with the Van Leer slope limiter and the HLLC Riemann solver provide second-order accuracy on the convective fluxes [23]. A second-order central-difference scheme is used to compute the viscous fluxes. The time integration is realized with the semi-implicit second-order ASIRK2 scheme [24] with a $2 \times 10^{-9}\,s$ time step.

The chemical kinetic scheme [25] comprises six species and seven reversible reactions and was already used for supersonic combustion [25][26] and detonation [12][27].

The Sigma subgrid turbulence approach of Nicoud et al. [28] models the unresolved turbulent structures. The meshes are composed of 100 µm tetrahedrons in the zone where propellant mixing and detonation propagation take place. The meshing is gradually coarsened towards the chamber exit ($y > 10$ mm). At the wall, layers of prisms are added to resolve the boundary layer. Table 1 gives information about the mesh refinement at the wall. The Celik criterion [29] was used to validate the spatial resolution of the 3D mesh. The Celik criterion is always above 0.8 in the present simulations, meaning that the mesh refinement is sufficient for LES simulations. Preliminary cold flow injection simulations were used to evaluate the turbulent integral length scale with two-point velocity correlations. The largest turbulent structures are resolved with more than 10 mesh cells, which seems sufficient for an LES simulation [30].

Regarding the boundary conditions, the total temperature and mass flow rate are set at the inlet of the manifolds connected to the tubes feeding the injector and used as buffer zones. The latter help to dissipate the shocks coming from the chamber and limit their influence on the inlet condition. The modeling of the friction is the no-slip condition, and that of the heat transfer is a fixed wall temperature arbitrarily set to 400 K. The pressure at the outlet is set to 1 atm, although in the present configuration, the flow at the outlet becomes supersonic when the simulation reaches steadiness.

2 Results and discussions

Table 1 shows the calculation cases and information about their resolution at the walls. The value of y^+ is calculated from Equation 1 and the local skin friction τ_w obtained in the simulation. The value of y^+ is not constant in the RDC, it increases in the detonation front. Table 1 shows the approximate value of y^+ away from the detonation front.

Table 1: LES cases

Case name	*Slip*	*Friction*	*Heat*	*Heat_ref*
Friction	No	Yes	Yes	Yes
Heat transfers	No	No	Yes	Yes
First cell size (µm)	10	10	10	1
y^+	1	1	1	0.1

$$y^+ = \frac{y}{\nu}\sqrt{\frac{\tau_w}{\rho}} \quad (1)$$

Figure 2 shows the instantaneous temperature field at the mid radius for the three cases *Slip*, *Friction*, and *Heat*. Overall, the resulting flows are very similar (Figure 2), with the typical triangular shape of the fresh mixture layer, and the oblique shock attached to the detonation front. At the chamber exit, the temperature is above 3000 K, indicating efficient heat release and good mixing in the chamber thanks to the *TripHy* injector. The fresh mixture layer is not continuous, with some burned gases trapped between adjacent propellant jets. This is particularly visible in Figure 2b) for the Friction case.

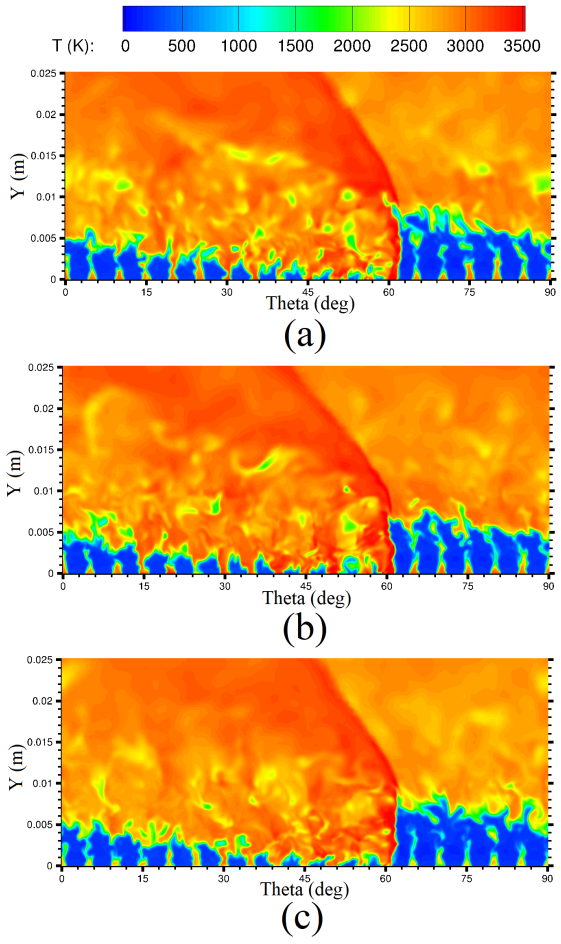

Figure 2: Temperature fields at the mid chamber radius for cases *Slip* (a), *Friction* (b) and *Heat* (c)

Figure 3 shows the 3D shape of the detonation wave 3 for the *Heat* case. The other cases result in a similar structure. The O_2 and H_2 injector plenums and the feed tubes are shown in purple and dark green, respectively. The pressure gradient norm $\|\vec{\nabla} P\|$ is shown in grayscale on the surfaces representing the injection wall and the mid radius. In these planes the iso-contour of the heat release $\dot{\omega}_T = 10^{12}$ W/m^3 is also shown in green. The current mesh resolution does not capture the inner structure of the detonation front. Nevertheless, the reaction zone is clearly coupled with the shock. The detonation front is mostly straight, except near the bottom of the chamber. In fact, at the bottom of the RDC, the injected propellants are not yet well mixed and the fresh mixture layer is discontinuous: the detonation passes through a succession of unmixed and burned gas zones. Successive shock reflections on the RDC walls are visible at the injection plane.

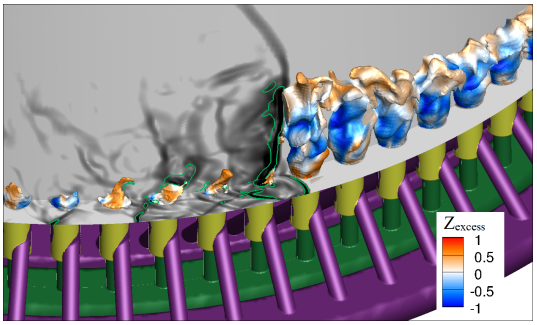

Figure 3: Pressure gradient (gray scale) at the mid chamber radius and the injection plane in case *Heat*, with the iso-contour $\dot{\omega}_T = 10^{12}$ W/m^3 in green. The iso-surface representing $T = 600$ K is colored-coded by Z_{excess}.

Figure 3 also shows the iso-surface T =600 K, colored with Z_{excess}, which visualizes the propellant jets. Positive (respectively negative) Z_{excess} corresponds to the volume fraction of H_2 (resp. O_2) in excess relative to stoichiometry. The red and blue zones indicate that the mixing of the propellants is not yet complete. A flame spontaneously forms at the interface of the fresh and burned gases. From Figure 3, for the*TripHy* injector, the flame at the fresh/burned gas interface is rich at the top of the fresh mixture layer and essentially lean everywhere else.

Equation 2 gives the detonation velocity (V_D) based on the pressure history recorded by numerical sensors located 1 mm downstream of the injection plane and at the mid chamber radius (R_{mid}). The quantities $n_{wave} = 4$ and τ_{sensor} denote the number of waves in the RDC and the time interval between two detonation passes indicated by strong pressure peaks. Five detonation periods and ten sensors are used to calculate the average detonation wave velocity.

$$V_D = \frac{2\pi R_{mid}}{n_{wave}\,\tau_{sensor}} \quad (2)$$

Table 2 summarizes the detonation wave velocities. The values are close to the theoretical CJ limit evaluated

from the injected mixture properties and the RDC average pressure. Experimental work is required to confirm these results.

Overall, the results confirm that viscous effects have a limited influence on the mean detonation velocity, about 1% for friction and 2% for heat transfer. The influence is larger on the standard deviation σ_D, which increases from 12 m/s in the *Slip* case to 20 m/s in the *Friction* and the *Heat* cases. Therefore, according to the present results, the overpredicted detonation velocity by simulations, compared to the experiments, does not seem to be due to neglecting wall friction and heat transfer.

Table 2: Mean value V_D and standard deviation σ_D of the detonation velocity

Case name	*Slip*	*Friction*	*Heat*
V_D (m/s)	2843	2859	2772
σ_D (m/s)	11.2	19.4	22.4

Figure 4 shows the variation of mixing efficiency in the fresh mixture layer produced by the injection element in front of the detonation front. The equation 3 defines the mixing efficiency, where *st* is the H_2 to O_2 mass fraction ratio at stoichiometry and S_y is the control volume section at coordinate y. The average mixing efficiency is obtained with 20 instantaneous fields. A control volume positioned just before the rotating detonation ensures tracking. The cases *Slip* and *Heat* result in very similar profiles of mixing efficiency. However, the mixing efficiency is lower for the *Friction* case and decreases faster at the top of the fresh mixture layer.

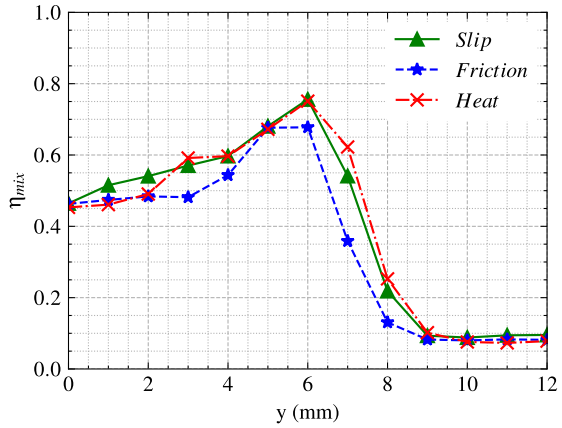

Figure 4: Mean mixing efficiency along the height of the fresh mixture layer

$$\eta_{mix}(y) = \frac{\iint_{S_y} \rho \min(Y_{H_2} + Y_{H_2}/st, Y_{O_2} + Y_{O_2} st) dS}{\iint_{S_y} \rho dS} \quad (3)$$

The deflagration losses are estimated by the method of Gaillard [31]. First, a control volume is positioned 1 mm in front of the detonation front. Its azimuthal and radial dimensions are the same as for an injection element. The height of the control volume y_{CV} is iterated until the equation 4 is satisfied. The equation 4 requires that the mass contained in the control volume $\iiint_{CV} \rho$ is equal to the mass injected during a period m_{inj}. In this equation, $\dot{m}_{tot}$ is the total mass flow rate in the RDC.

Case	*Slip*	*Friction*	*Heat*
y_{CV} (mm)	10	11	9
m_{mix}/m_{inj} (%)	69	61	70
m_{unmix}/m_{inj} (%)	10	11	11
m_{burned}/m_{inj} (%)	21	28	19

Table 3: Fresh mixture layer properties before the detonation

$$\iiint_{CV} \rho dV = m_{inj} = \tau \frac{\dot{m}_{tot}}{n_{inj}} = \frac{2\pi R_{mid}}{V_D n_{wave}} \frac{\dot{m}_{tot}}{n_{inj}} \quad (4)$$

In this control volume, the composition of the computational cells is divided into three categories: the perfectly mixed propellant mass m_{mix}, the unmixed propellant mass m_{unmix}, and the burned gas mass m_{burned}. By dividing each by their sum m_{inj}, one can evaluate the deflagration losses and the average mixing efficiency in the control volume. Table 3 shows the results for the three simulation cases.

The three cases show the same level of unmixing (10%). Regarding the fraction of mixed propellants, it is about 70% for the *Slip* and *Heat* cases, but it decreases to 61% in the *Friction* simulation. The decrease in mixing efficiency is due to higher parasitic deflagration consuming the mixed propellants as the burned gas fraction reaches 28% in the *Friction* case.

Increased deflagration losses can be related to several effects. For example, flow shear near the walls can promote turbulence development and increase flame surface density. Wall friction also slows the flow near the wall, which increases the pressure and temperature near the injector. Higher temperature increases the preheating of propellants and, thus, deflagration losses.

In the case of *Heat*, thermal losses at the wall cool the burned gases, so the flame is slower and may even be quenched. All these factors can explain the lower deflagration losses in this case.

Overall, the present *TripHy* injector shows good performance with more than 60% of the injected propellants mixed at stoichiometry for less than 30% of the deflagration losses according to the present method. This promising performance is one of the main factors for the high detonation velocity in the simulations.

Figure 5 shows the time and azimuthally averaged wall heat flux for the *Heat* and *Heat_ref* cases. In *Heat_ref*, the first cell at the wall is 1 µm thick.

A high heat flux - approximately 15 MW/m² - is obtained between 0 and 8 mm, which corresponds to the thickness of the fresh mixing layer discussed in the previous section. The heat flux then drops rapidly to 7 MW/m² at 10 mm above the injector. The heat flux then decreases almost linearly towards the chamber exit. The

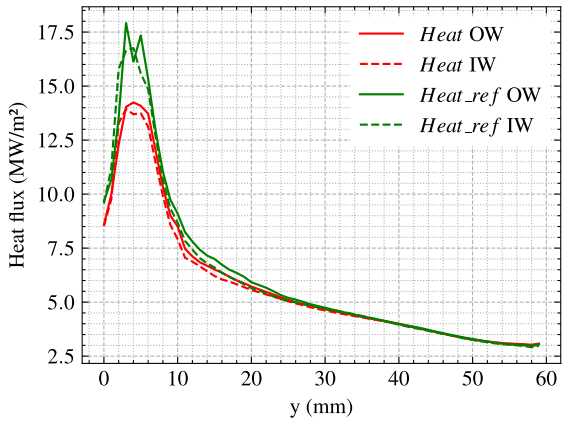

Figure 5: Time- and azimuthally- averaged heat flux at the outer (OW) and inner (IW) walls

inner wall (IW) appears to have a lower heat load because the chamber curvature induces a stronger detonation at the outer wall (OW). The effect of mesh refinement is high in the detonation propagation zone, i.e., where the pressure and flow velocity are larger: the maximum heat flux increases from 14 MW/m² to 17 MW/m². This effect is smaller in the rest of the chamber. The y^+ value is highly variable in the RDC. For example, y^+ decreases from 50 in the *Heat* case to 5 in the *Heat_ref* case in the detonation front. Therefore, the coarser mesh underestimates the heat flux in the detonation zone. An even finer mesh may be required to resolve the near-wall gradients in the detonation front.

The simulated heat load indicates that long-term operation requires a cooling system, even at low chamber pressures. The detonation propagation region is the most critical zone for cooling. Integrating the wall heat flux over the wall surfaces gives a thermal power loss of 9.9% of the lower heating value (LHV) for the *Heat* case and 10.6% for the *Heat_ref* case. This result is 2% higher than that obtained by Theuerkauf et al. [10] for a H_2/air RDC. In a rocket-type RDC, regenerative cooling could use these losses to preheat and pre-evaporate the propellants before injection, as in conventional rocket engines.

Conclusions

This study presents a sensitivity analysis of the viscous wall interactions in an RDC based on high-fidelity simulations. The calculations were performed using ONERA's CEDRE software. The simulations indicate that the *TripHy* injector produces good propellant mixing, as the simulated detonation velocity is close to its theoretical D_{CJ} value. The results show that viscous effects only weakly influence the detonation velocity. They also indicate that the detonation propagation zone experiences the highest heat load and suggest that a cooling system is necessary for operational RDCs. Highly refined meshes are required to accurately predict the heat flux in this region. Experimental work is now required to validate these numerical results.

Acknowledgements

This study was co-funded by the General Scientific Direction of ONERA and the Nouvelle-Aquitaine Region under the grant agreement n°15833220.

The authors thank Patrick Berterretche and Nicolas Laroche for their help in designing the *TripHy* injector.

References

[1] M. Salvadori, P. Tudisco, D. Ranjan, and S. Menon, Numerical investigation of mass flow rate effects on multiplicity of detonation waves within a h2/air rotating detonation combustor, *International Journal of Hydrogen Energy* **47**, 4155 (2022).

[2] F. A. Bykovskii and E. F. Vedernikov, Heat fluxes to combustor walls during continuous spin detonation of fuel-air mixtures, *Combustion, Explosion, and Shock Waves* **45**, 70 (2009).

[3] P. Wolański, in *Applied Mechanics and Materials* (Trans Tech Publ, 2015), vol. 782, 3–12.

[4] A. Naples, J. Hoke, R. T. Battelle, M. Wagner, and F. R. Schauer, in *55th AIAA Aerospace sciences meeting* (2017), 1747.

[5] M. L. Fotia, F. Schauer, T. Kaemming, and J. Hoke, Experimental study of the performance of a rotating detonation engine with nozzle, *Journal of Propulsion and Power* **32**, 674 (2016).

[6] S. Frolov, V. Aksenov, V. Ivanov, S. Medvedev, I. Shamshin, N. Yakovlev, and I. Kostenko, in *Doklady Physical Chemistry* (Springer, 2018), vol. 478, 31–34.

[7] D. Davidenko, I. Gökalp, and A. Kudryavtsev, in *15th AIAA International Space Planes and Hypersonic Systems and Technologies Conference* (2008), 2680.

[8] S. Randall, V. Anand, A. C. St. George, and E. J. Gutmark, in *53rd AIAA aerospace sciences meeting* (2015), 0880.

[9] K. Goto, J. Nishimura, A. Kawasaki, K. Matsuoka, J. Kasahara, A. Matsuo, I. Funaki, D. Nakata, M. Uchiumi, and K. Higashino, Propulsive performance and heating environment of rotating detonation engine with various nozzles, *Journal of Propulsion and Power* **35**, 213 (2019).

[10] S. W. Theuerkauf, F. Schauer, R. Anthony, and J. Hoke, in *53rd AIAA Aerospace sciences meeting* (2015), 1603.

[11] S. Zhou, H. Ma, C. Liu, C. Zhou, and D. Liu, Experimental investigation on the temperature and heat-transfer characteristics of rotating-detonation-combustor outer wall, *International Journal of Hydrogen Energy* **43**, 21079 (2018).

[12] T. Gaillard, D. Davidenko, and F. Dupoirieux, Numerical simulation of a rotating detonation with a realistic injector designed for separate supply of gaseous hydrogen and oxygen, *Acta Astronautica*

141, 64 (2017).

[13] X.-Y. Liu, Y.-L. Chen, Z.-J. Xia, and J.-P. Wang, Numerical study of the reverse-rotating waves in rotating detonation engine with a hollow combustor, *Acta Astronautica* **170**, 421 (2020).

[14] P. Pal, G. Kumar, S. A. Drennan, B. A. Rankin, and S. Som, Multidimensional numerical modeling of combustion dynamics in a non-premixed rotating detonation engine with adaptive mesh refinement, *Journal of Energy Resources Technology* **143** (2021).

[15] S. Prakash, V. Raman, C. F. Lietz, W. A. Hargus Jr, and S. A. Schumaker, Numerical simulation of a methane-oxygen rotating detonation rocket engine, *Proceedings of the Combustion Institute* **38**, 3777 (2021).

[16] P. C. Nassini, Ph.D. thesis, University of Florence (2022).

[17] P. A. Cocks, A. T. Holley, and B. A. Rankin, High fidelity simulations of a non-premixed rotating detonation engine, *54th AIAA aerospace sciences meeting* 0125 (2016).

[18] Y. Wang, J. Wang, and W. Qiao, Effects of thermal wall conditions on rotating detonation, *Computers & fluids* **140**, 59 (2016).

[19] K. Wu, L. Zhang, M.-Y. Luan, and J.-P. Wang, Effects of isothermal wall boundary conditions on rotating detonation engine, *Combustion Science and Technology* **193**, 211 (2021).

[20] P. A. Cocks, A. T. Holley, C. B. Greene, and M. Haas, in *53rd AIAA Aerospace Sciences Meeting* (2015), 1823.

[21] B. Gelfand, S. Frolov, and M. Nettleton, Gaseous detonations—a selective review, *Progress in energy and combustion science* **17**, 327 (1991).

[22] A. Higgins, Steady one-dimensional detonations, *Shock Waves Science and Technology Library, Vol. 6: Detonation Dynamics* 33–105 (2012).

[23] A. Refloch, B. Courbet, A. Murrone, P. Villedieu, C. Laurent, P. Gilbank, J. Troyes, L. Tessé, G. Chaineray, J. Dargaud, et al., CEDRE Software, *Aerospace Lab* p. 1–10 (2011).

[24] X. Zhong, Additive semi-implicit runge–kutta methods for computing high-speed nonequilibrium reactive flows, *Journal of Computational Physics* **128**, 19 (1996).

[25] D. Davidenko, I. Gökalp, E. Dufour, and P. Magre, in *12th AIAA international space planes and hypersonic systems and technologies* (2003), 7033.

[26] C. Fureby, K. Nordin-Bates, K. Petterson, A. Bresson, and V. Sabelnikov, A computational study of supersonic combustion in strut injector and hypermixer flow fields, *Proceedings of the Combustion Institute* **35**, 2127 (2015).

[27] D. M. Davidenko, I. Gökalp, and A. N. Kudryavtsev, in *West-East High Speed Flow Field Conference* (2007).

[28] F. Nicoud, H. B. Toda, O. Cabrit, S. Bose, and J. Lee, Using singular values to build a subgrid-scale model for large eddy simulations, *Physics of fluids* **23**, 085106 (2011).

[29] I. Celik, Z. Cehreli, and I. Yavuz, Index of resolution quality for large eddy simulations, *Journal of fluids engineering* **127**, 949 (2005).

[30] L. Davidson, in *Quality and Reliability of Large-Eddy Simulations II* (Springer, 2011), 269–286.

[31] T. Gaillard, Ph.D. thesis, Université Paris Saclay (COmUE) (2017).